MATEC Web of Conferences **33**, 03018 (2015)
DOI: 10.1051/matecconf/20153303018
© Owned by the authors, published by EDP Sciences, 2015

Deformation behavior after stress-induced martensite transformation in a Ti-50.8 at.% Ni alloy

Xiebin Wang, Bert Verlinden and Jan Van Humbeeck[a]

Department of Materials Engineering, KU Leuven, Kasteelpark Arenberg 44 bus 2450, B3001 Heverlee, Belgium.

Abstract. In this study, the deformation behavior of a Ti-50.8 at.% Ni thin wire, which was subjected to different heat treatments, was investigated by means of uniaxial tensile tests. Considerable ductility (tensile elongation >50%) and a large variation of the stress-strain relations are observed after different heat treatments, especially in the stage after the stress-induced martensite transformation plateau. A possible explanation for the observed phenomenon is discussed in this work.

1 Introduction

Near equiatomic NiTi shape memory alloys are attracting widespread interest for practical applications not only as functional materials but also as engineering materials, due to their considerable ductility (tensile strain >30% [1,2]) and strength (ultimate tensile stress >1 GPa after proper treatments [2,3]). However, it is unusual for the B2 structured NiTi alloy to show a very good ductility, as the lattice structure can only provide three independent slip systems [1]. B2 structured intermetallics (e.g. NiAl, CuZn) are very important materials, due to their unique physical and mechanical properties [4,5], but further application of these alloys is limited by their poor ductility [6]. Therefore, understanding the origin of the good ductility of NiTi alloys may provide new approaches to improve the ductility of other intermetallic materials.

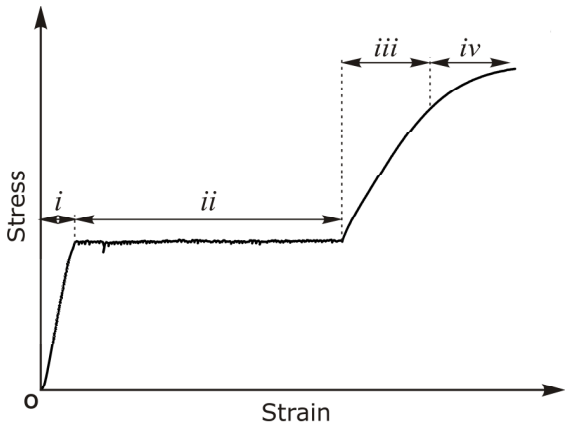

Figure 1. Schematic illustration of the various stages during tensile deformation of NiTi alloys, showing the stress-induced martensite transformation during loading (for details see text).

As illustrated in Fig. 1, with increasing tensile load, NiTi alloys with initial B2 austenite (A) phase may undergo the following four stages: (*i*) elastic deformation of the austenite phase; (*ii*) stress-induced martensite (SIM) transformation; (*iii*) elastic and (*iv*) plastic deformation of the B19' martensite (M) phase obtained in stage *ii*. The mechanism of SIM transformation (stage *ii*) has been well studied [7,8]. However, there has been little discussion on the deformation behavior in stage *iii* and *iv*.

In this work, different deformation behavior is observed in a Ti-50.8 at.% Ni thin wire after different heat treatments. A possible explanation for the variation of the stress-strain response is discussed and particular attention is focused on the link between the microstructure and the deformation behavior in stage *iv*.

2 Experimental procedure

A commercial NiTi thin wire (diameter 50 μm) with a nominal composition of Ti-50.8 at.% Ni was used. The as-received wire was produced by room-temperature wire drawing with a final cold deformation of around 25%. The as-received wire was annealed at 873 K for 30 min in argon atmosphere, followed by water quenching at room temperature. The annealed samples were further aged for 8 hours at 523 and 723 K, respectively, in argon atmosphere, followed by furnace cooling to room temperature.

The grain size and crystallographic orientation of the sample annealed at 873 K for 30 min were characterized using electron backscattered diffraction (EBSD), which was performed on an FEI Nova 600 NanoLab instrument equipped with a TSL/EDAX system. The surface for EBSD measurement, which is perpendicular to the wire axis, was prepared using a JEOL IB-09010CP cross-section polisher. The transformation behavior was

[a] Corresponding author: Jan.Vanhumbeeck@mtm.kuleuven.be

This is an Open Access article distributed under the terms of the Creative Commons Attribution License 4.0, which permits unrestricted use distribution, and reproduction in any medium, provided the original work is properly cited.

Article available at http://www.matec-conferences.org or http://dx.doi.org/10.1051/matecconf/20153303018

characterized by differential scanning calorimetry (DSC) in a TA Q2000 calorimeter between 123 and 423 K with a heating/cooling rate of 10 K/min. The tensile tests were performed at a constant strain rate of 1.67×10^{-4} s^{-1} using a TA Q800 dynamic mechanical analyzer. The length of the samples was 10.5 ± 0.5 mm.

3 Results and discussion

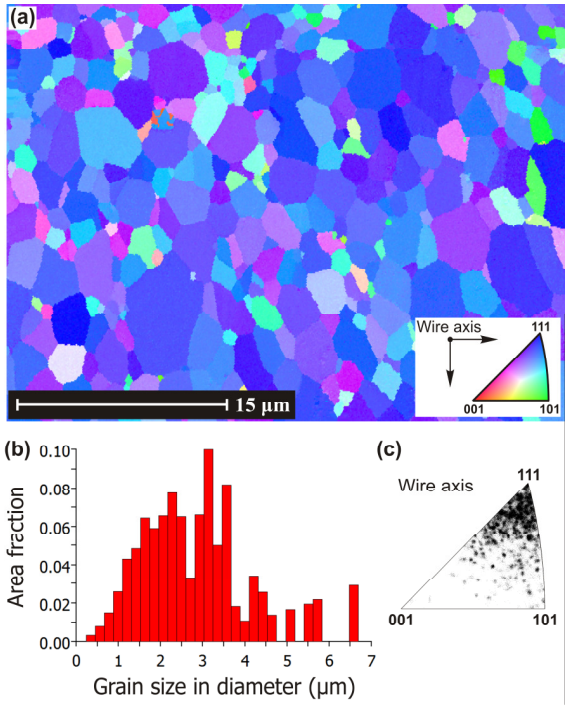

Figure 2. (a) EBSD orientation map and (b) grain size distribution histogram of the sample annealed at 873 K for 30 min; (c) inverse pole figure of the crystallographic orientations with the reference of wire axis. The observed surface is normal to the wire axis.

Figure 2a shows the EBSD map of the as-received Ti-50.8 at.% Ni wire after annealing at 873 K for 30 min. Fully recrystallized equiaxed grains with an average grain size of 1.7 μm are revealed. The grain size distribution histogram shown in Fig. 2b indicates that most of the grains have a diameter < 3.5 μm. A strong <111> fiber texture is revealed by the inverse pole figure with reference to the wire axis, as shown in Fig. 2c. The transformation strain of NiTi alloys depends strongly on the crystallographic orientation, and the maximum value can be obtained near the $<111>_{B2}$ orientation [7,9]. Therefore, the strong <111> fiber texture provides a large transformation strain in the axial direction of the wire.

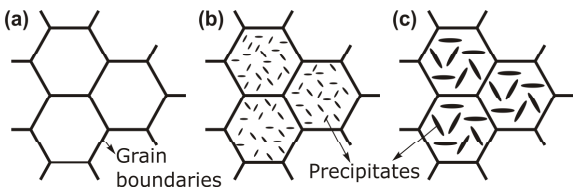

Figure 3. Schematic illustration of the microstructure after (a) annealing at 873 K for 30 min, followed by aging at (b) 523 K and (c) 723 K for 8 hours (for details see text).

After annealing at 873 K for 30 min, the Ti-50.8 at.% Ni wire was further aged for 8 hours at 523 and 723 K, respectively. The microstructural difference between the samples before and after aging treatment is illustrated in Fig. 3. After annealing at 873 K for 30 min, the samples show fully recrystallized microstructure with an average grain size of 1.7 μm, as shown in Fig. 2 and 3a. The grain size is considered to remain unchanged during aging treatment, as the aging temperatures (523 and 723 K) are much lower than the recrystallization temperature (823-873 K [2,10]). Ni_4Ti_3 precipitates with a length of around 5 nm can be introduced by aging at 523 K (Fig. 3b), as discussed in our previous work [11,12]. Large Ni_4Ti_3 precipitates are expected in the sample after aging at 723 K for 8 hours [13], as illustrated in Fig. 3c. As the grain size is small (average grain size of 1.7 μm), it is considered that the precipitates distribute homogenously in the matrix after aging at both 523 and 723 K[11,12,14], as evidenced by the absence of the multi-stage martensitic transformation, as shown in Fig. 4 [14]. The multi-stage martensitic transformation has been observed frequently in the samples with large grains after aging treatments [15–17].

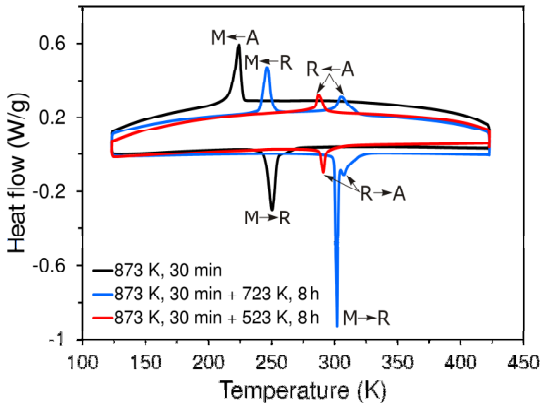

Figure 4. DSC curves of a Ti-50.8 at.% Ni alloy after annealing at 873 K for 30 min, followed by aging for 8 hours at 523 and 723 K, respectively.

The transformation behavior of the samples after annealing and aging treatments is shown in Fig. 4. After annealing at 873 K for 30 min, the sample shows a normal A↔M transformation with the B19' martensite transformation start temperature (M_s) at 228 K. After aging at 523 K for 8 hours, a one-stage A↔R transformation is observed, as shown in Fig. 4. This is due to the fact that nano-scaled Ni_4Ti_3 precipitates can distribute homogeneously in the sample with micron-sized grains [14], which prohibits the occurrence of multi-stage martensitic transformation as well as supresses the B19' martensite transformation [11,12,14]. Two-stage A↔R↔M transformation with M_s at 251 K is observed in the sample aged at 723 K for 8 hours.

Figure 5 shows the stress-strain curves of the Ti-50.8 at.% Ni thin wire after the different heat treatments. With increasing tensile load, all the samples undergo SIM transformation (i.e. stage *ii* in Fig. 1), leading to a stress plateau, as shown in Fig. 5a. The difference in the plateau stress is due to the different martensite transformation

temperatures between the samples after different heat treatments (Fig. 4), according to the Clausius-Clapeyron type relation between the critical stress and temperature of SIM transformation [18]. It is noteworthy that for the sample aged at 523 K a SIM transformation is recorded at high stress levels, although no martensite transformation peak could be observed by DSC. The differences in the transformation strain (i.e. the length of the transformation plateau) is due to the different volume fraction of Ni_4Ti_3 precipitates, as increasing precipitation volume fraction results in decreasing transformation strain [19].

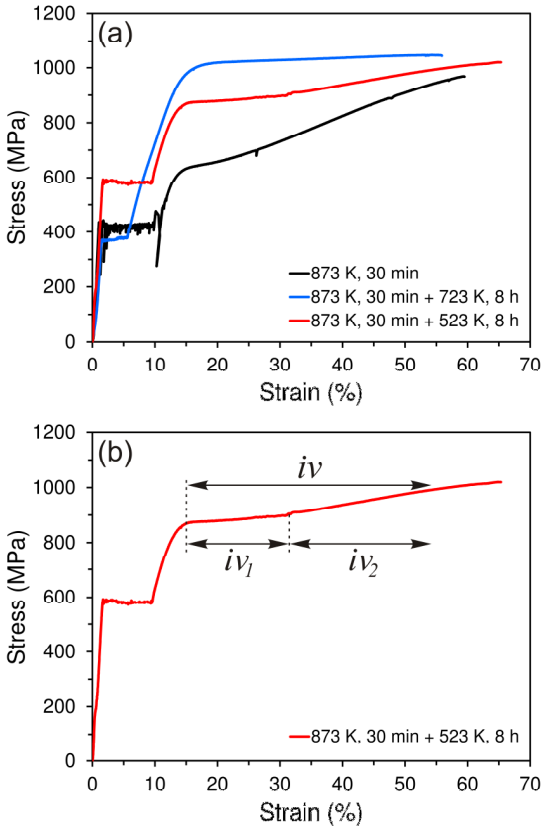

Figure 5. (a) Stress-strain curves of a Ti-50.8 at.% Ni wire after different heat treatments; (b) the martensite plastic deformation part (stage *iv*) can be divided into two stages. Stage iv_1 is featured as very low strain hardening rate as compared with that of stage iv_2.

It is interesting to observe that the stress-strain response during the plastic deformation of the martensite phase (i.e. stage *iv* in Fig. 1) varies a lot between the samples with different heat treatments, as shown in Fig. 5a. The as-annealed sample shows that the stress increases gradually with increasing strain in stage *iv*. After aging at 723 K for 8 hours, the sample shows barely a strain hardening effect. For the sample aged at 523 K for 8 hours, the stress-strain curve in stage *iv* can be divided into two stages, as indicated in Fig. 5b. Stage iv_1 features a very low strain hardening rate, while stage iv_2 has a higher strain hardening rate than that of stage iv_1.

The microstructural differences are considered as the main reason for the different deformation behavior shown in Fig. 5a. Due to the microstructural heterogeneity (e.g. between the vicinity of precipitates and the region away from precipitates), some of the austenite phase may not transform into B19' martensite in stage *ii*, but in stage *iii* or even in stage *iv*. As shown in Fig. 6, it is assumed that the austenite matrix can be divided into the following three parts: (a) "normal" austenite, which transforms into B19' martensite in stage *ii*; (b) "residual" austenite, which transforms into B19' martensite in stage *iii*; and (c) "lazy" austenite, which transforms into B19' martensite in stage iv_1.

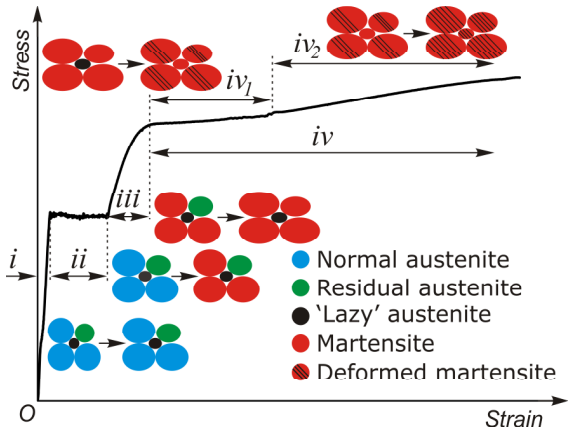

Figure 6. Schematic explanation on the deformation behavior of NiTi alloys, which show considerable elongation strain (for details see text).

Therefore, the different stages of the strain-stress curve shown in Fig. 5a may be explained as follows (Fig. 6):

Stage *i*: elastic deformation of austenite phase. The stress-induced R-phase or R-phase reorientation may occur in this stage [20].

Stage *ii*: stress-induced martensite transformation. The "normal" austenite transforms into B19' martensite in this stage. However, the "residual" and "lazy" austenite still remains in the austenite phase.

Stage *iii*: elastic deformation of the B19' martensite phase obtained in stage *ii*. The "residual" austenite transforms into martensite in this stage, leading to a non-linear stress-strain relation. Moreover, elastic deformation of the Ni_4Ti_3 precipitates may also occur in this stage, especially in the sample aged at 723 K, which has a high volume fraction of precipitates.

Stage iv_1: plastic deformation of the martensite obtained in stage *ii* and *iii*. The "lazy" austenite transforms into martensite in this stage. The transformation may give rise to the "transformation induced plasticity" effect [21]. The length of this stage may depend on the volume fraction of "lazy" austenite.

Stage iv_2: Further plastic deformation of martensite phase.

However, further investigation, especially the *in situ* observation, is required to reveal the microstructure change during tensile deformation.

4 Conclusions

In this work, a Ti-50.8 at.% Ni wire was subjected to different heat treatments. Considerable ductility (tensile elongation >50%) is observed in the samples after heat treatments. The different deformation behavior is

discussed based on the differences in microstructure of the samples after different heat treatments. Further investigations are required to study the deformation mechanism and to reveal the origin of considerable ductility of NiTi alloys, and thus to improve the ductility of other B2 structured intermetallics.

Acknowledgements

This work was supported by the Research Foundation Flanders (FWO) under Grant No. G036615N. Xiebin Wang wishes to thank the China Scholarship Council for financial support.

References

1. T.W. Duerig, Mater. Sci. Eng. A **438–440**, 69 (2006)
2. S. Miyazaki, Y. Kohiyama, K. Otsuka, T.W. Duerig, Mater. Sci. Forum **56–58**, 765 (1990)
3. X. Wang, B. Amin-Ahmadi, D. Schryvers, B. Verlinden, J. Van Humbeeck, Mater. Sci. Forum **738–739**, 306 (2013)
4. G. Sauthoff, *Intermetallics* (Wiley-VCH, Weinheim, 1995)
5. N.S. Stoloff, C.T. Liu, S.C. Deevi, Intermetallics **8**, 1313 (2000)
6. I. Baker, Scripta Mater. **41**, 409 (1999)
7. K. Otsuka, X. Ren, Prog. Mater. Sci. **50**, 511 (2005)
8. Y. Liu, Acta Mater. **95**, 411 (2015)
9. T. Saburi, M. Yoshida, S. Nenno, Scripta Mater. **18**, 363 (1984)
10. Y. Liu, P.G. McCormick, Acta Metall. Mater. **38**, 1321 (1990)
11. X. Wang, K. Li, D. Schryvers, B. Verlinden, J. Van Humbeeck, Scripta Mater. **72–73**, 21 (2014)
12. X. Wang, S. Kustov, K. Li, D. Schryvers, B. Verlinden, J. Van Humbeeck, Acta Mater. **82**, 224 (2015)
13. J. Khalil-Allafi, G. Eggeler, A. Dlouhy, W.W. Schmahl, Ch. Somsen, Mater. Sci. Eng. A **378**, 148 (2004)
14. X. Wang, C. Li, B. Verlinden, J. Van Humbeeck, Scripta Mater. **69**, 545 (2013)
15. J.I. Kim, Y. Liu, S. Miyazaki, Acta Mater. **52**, 487 (2004)
16. G. Fan, W. Chen, S. Yang, J. Zhu, X. Ren, K. Otsuka, Acta Mater. **52**, 4351 (2004)
17. J. Khalil-Allafi, A. Dlouhy, G. Eggeler, Acta Mater. **50**, 4255 (2002)
18. P. Wollants, J.R. Roos, L. Delaey, Prog. Mater. Sci. **37**, 227 (1993)
19. C. Efstathiou, H. Sehitoglu, Scripta Mater. **59**, 1263 (2008)
20. S. Miyazaki, K. Otsuka, Metall. Trans. A **17**, 53 (1986)
21. F.D. Fischer, G. Reisner, E. Werner, K. Tanaka, G. Cailletaud, T. Antretter, Int. J. Plast. **16**, 723 (2003)